Stereochemical Features of the (2 + 2) Cycloaddition Reactions of Chiral Allenes. 2. Cycloaddition of Enantioenriched 1,3-Dimethylallene with the 1,2-Disubstituted Alkenes *N*-Phenylmaleimide and Dimethyl Fumarate

Daniel J. Pasto* and Kiyoaki D. Sugi

Department of Chemistry and Biochemistry, University of Notre Dame, Notre Dame, Indiana 46556

Received March 18, 1991

The cycloaddition reaction of *N*-phenylmaleimide (NPMI) with an excess of enantioenriched 1,3-dimethylallene (13DMA) has been carried out with varying initial enantiomeric excesses (ee's) of the 13DMA and differing concentrations of the reactants. The recovered unreacted 13DMA showed no loss in ee. The four cycloadducts have been separated by HPLC, and their ee's have been determined by the use of a chiral NMR chemical shift reagent. Two of the cycloadducts have retained ~80% of the ee of the starting 13DMA, one ~50%, and the fourth ~10%. Molecular modeling calculations have been carried out on the conformational energy surface for the approach of reactant models to the activated complexes for diradical intermediate formation, and on models for the diradical intermediates. A mechanism is proposed for the formation of the diradical intermediates and the cycloadducts involving three separate minimum-energy reaction channels for the formation of specific conformations of the diradical intermediates which undergo ring closure to specific cycloadducts. These minimum-energy reaction channels differ in the extent of the facial selectivity of attack on the NPMI during the irreversible formation of the diradical intermediates. The cycloaddition of 13DMA with dimethyl fumarate (DMFM) produces two major cycloadducts which have been formed involving >96 and >70% transfer of the ee of the starting 13DMA. Two very minor cycloadducts are also formed, one possessing ~74% of the ee of the starting 13DMA with the other minor cycloadduct being formed in such small quantities that is isolation and measurement of its ee could not be accomplished. Molecular modeling calculations have been carried out on the conformational energy surface of the two reactants in approaching the activated complexes for diradical intermediate formation and on the conformational preferences of the diradical intermediates. The detailed stereochemical analysis of the formation of the cycloadducts suggests that there are two major minimum-energy reaction channels involved in diradical intermediate and cycloadduct formation arising from the same low-energy conformation for approach of the reactants to two different activated complexes and diradical intermediates.

Introduction

In the preceding paper in this series the stereochemical features of the (2 + 2) diradical intermediate cycloaddition reactions of symmetrically and unsymmetrically substituted chiral allenes with 1,2- and 1,1-disubstituted and monosubstituted radicophiles were discussed, and the stereochemical results of the cycloaddition reactions of enantioenriched 13DMA with the monosubstituted radicophiles acrylonitrile and methyl acrylate were described.[1] The results of those studies indicated that a substantial degree of the enantiomeric excess (ee, up to 39%) of the 13DMA is transferred to the intermediate diradicals despite the fact that a stereogenic center is not formed at one of the carbon atoms involved in the C–C bond forming process. The diradical intermediates formed in these cycloaddition reactions are chiral by virtue of their conformation about the newly formed C–C bond and the stereogenic radical center.[1,2] Molecular modeling calculations on the conformations for the approach of the reactants to the activated complexes for diradical intermediate formation allowed for the prediction of the absolute configurations of the diradical intermediates and, ultimately, in the cycloadducts. The predicted absolute configurations derived from the molecular modeling calculations[1] were completely consistent with the experimental observations of Baldwin and Roy,[3] who reported that the cycloaddition of enantioenriched (*R*)-(−)-13DMA with acrylonitrile produced four cycloadducts which possessed the *R* configuration at C_2 of the four-membered ring. In the present paper we wish to present the results derived from studies on the cycloaddition reactions of enantioenriched (*S*)-(+)-13DMA with *N*-phenylmaleimide (NPMI) and dimethyl fumarate (DMFM).

In the formation of the diradical intermediates in the reactions of 13DMA and a 1,2-disubstituted radicophile the axial chirality of the 13DMA is transferred to the newly formed stereogenic carbon atoms in the intermediates represented as **1** and **2**. **1** and **2** differ stereochemically in a very subtle manner. There is a local, vertical plane of symmetry in the allyl-radical portion of **1**, whereas in **2** there is no local, vertical plane of symmetry in the allyl-radical portion of the intermediate. Thus, **1** and **2** differ in their total "intrinsic asymmetry"[1] and would be expected to be formed with different extents of transfer of the ee (degree of asymmetric induction) of the 13DMA to the diradical intermediates and on to the cycloadducts. However, if the formation of **1** and **2** is reversible and if the extent of the transfer of the ee of the 13DMA to **1** and **2** is less than 100%, the recovered, unreacted 13DMA will show a loss in ee, and the ee's of the cycloadducts will decrease with reaction time. Such data would provide for a very sensitive probe for detecting the reversibility in the formation of the diradical intermediates. The ee's of the diradical intermediates are locked in; i.e., there is no mechanism for their racemization, and the extent of transfer of the ee of the 13DMA to the diradical intermediates is directly indicated by the ee's of the cycloadducts. The results reported herein indicate that the formation of the diradical intermediates is irreversible and that at least three reaction channels are involved in diradical formation, which differ in the extent of transfer of the ee of the 13DMA to the diradical intermediates and cycloadducts.

Results and Discussion

Cycloaddition of Enantioenriched (*S*)-(+)-13DMA with NPMI. The cycloaddition reactions of (*S*)-(+)-

(1) Pasto, D. J.; Sugi, K. D. *J. Org. Chem.* **1991**, *57*, 3795.
(2) Mislow, K.; Siegel, J. *J. Am. Chem. Soc.* **1984**, *106*, 3319.
(3) Baldwin, J. E.; Roy, U. V. *Chem. Commun.* **1969**, 1225.

0022-3263/91/1956-6216$02.50/0

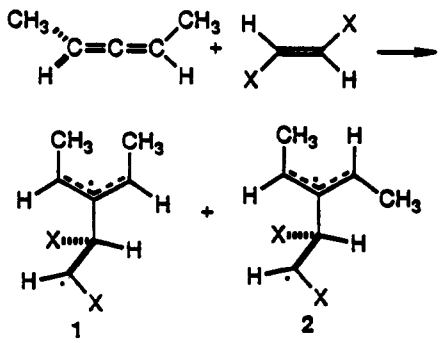

1 2

13DMA with NPMI were carried out in toluene-d_8 solution in sealed NMR tubes using a 100% excess of the 13DMA. The tubes were heated in a sand bath at 160 °C and were periodically monitored by NMR spectroscopy for the extent of reaction. The NMR spectra recorded at intermediate times showed the formation of only the four previously characterized cycloadducts,[4] whose ratio did not change during the course of the reaction. After the NPMI had completely reacted, the tubes were opened and the volatiles were removed on a vacuum line. The unreacted 13DMA was recovered from the volatile fraction by preparative GLC, and its rotation was recorded. The mixture of the four cycloadducts was separated by preparative HPLC. The ee's of the individual cycloadducts have been determined by the use a chiral ytterbium NMR chemical shift reagent employing double resonance techniques giving base-line resolution of the ring methyl or vinyl methyl resonances in the diastereomeric complexes. A typical NMR spectrum recorded under such conditions is shown in Figure 1. When a mixture of 3 and 4 was heated at 160 °C in toluene-d_8 for 3 days there was no change in the ratio of 3 to 4 or their ee's nor was there any formation of 5 and 6.

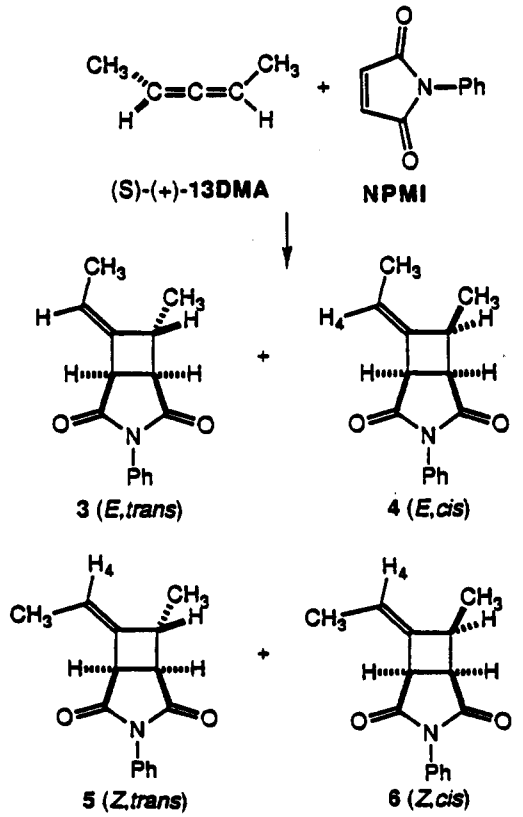

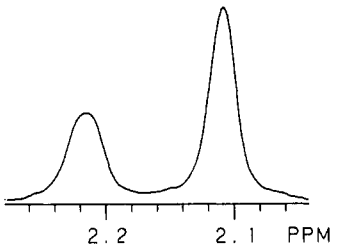

Figure 1. Partial NMR spectrum of the vinyl methyl region of cycloadduct 4 in the presence of Yb(fhc)$_3$ with double resonance of the vinyl proton.

Table I. Percent ee's of the Starting and Recovered (*S*)-(+)-13DMA and the Percent Yields and ee's of the Cycloadducts 3–6

reactant/cycloadduct	% yield[b]	% ee's[a] run 1	run 2	run 3	run 4[c]	run 5
13DMA (start)		28.1	30.3	30.3	32.3	47.9
13DMA (recd)		27.1	*d*	29.2	*d*	43.3
3	32	2.9	2.2	2.0	2.8	7.0
4	33	23.4	21.0	*d*	25.8	36.6[e]
5	29	13.9	14.8	15.0	12.8	24.4
6	6	25.8	25.4	25.0	*d*	37.7

[a] Estimated maximum ±0.6%. [b] Variation in relative yields from run to run of ±2%. [c] Five-fold dilution of the concentrations used in runs 1–3 and 5. [d] Either impurity or an inadequate quantity of sample prevented determination of the value. [e] Ozonolysis to the corresponding substituted cyclobutanone followed by ee analysis with a chiral europium NMR chemical shift reagent gave an ee value of 36.2%.

The results of several runs carried out with differing ee's of the starting 13DMA and reactant concentrations are given in Table I. The relative yields and the relative extents of the transfer of the ee of the 13DMA to the individual cycloadducts remains remarkably constant for the five experiments. The results suggest that there is no chiral medium effect and that the cycloaddition process is not more kinetically complicated than originally assumed (i.e., a bimolecular, rate-determining formation of a diradical intermediate). In three runs the recovered 13DMA showed no loss in ee within experimental error of the optical rotation measurements.

In view of the fact that the ee's of the individual cycloadducts are less than that of the starting 13DMA and that no racemization of the 13DMA had occurred during the reaction, it must be concluded that the formation of the diradical intermediate(s) is irreversible. In addition, had a single minimum-energy reaction channel given rise to a single diradical intermediate which could then undergo ring closure to produce all four cycloadducts, all four of the cycloadducts would have possessed the same ee. The formation of the four cycloadducts possessing at least three experimentally different ee's demands that at least three discrete minimum-energy reaction channels are involved in cycloadduct formation, each of which gives rise to a discreet cycloadduct, or in one case possibly a pair of cycloadducts.

In order to gain a possible understanding of these results we have carried out extensive molecular modeling calculations on the conformational energy surface of the reactants in approaching the activated complexes for *re* and *si* face attack on NPMI by (*S*)-(+)-13DMA and on models for the diradical intermediates using the MME and "molecular fitting" routines of the Chem-X suite of programs.[5] (In these calculations the phenyl group of the

(4) Pasto, D. J.; Sugi, K. D. *J. Org. Chem.* **1991**, *57*, 3781.

(5) Chem-X, distributed by Chemical Design, Ltd., Oxford, England.

NPMI and the anti methyl groups of the allyl radical portions of the intermediates have been replaced by a hydrogen atom.) The structures of the model for NPMI and the (*S*)-(+)-13DMA were first optimized and were then "docked" in such a manner that the axes of the two 2p AO's undergoing bond formation were coincident with a C_1–$C_{1'}$ separation distance of 2.0 Å. The MME energy surface was then computed for a 360° rotation about the C_1–$C_{1'}$ bond.[6] The resulting energy profiles for the *si* and *re* approach to the NPMI are shown in Figures 2 and 3. The conformational energy surfaces are quite complex, having six maxima and six minima. The lowest energy point on the two profiles is for *si* approach with a C_2–C_1–$C_{1'}$–$C_{2'}$ dihedral angle of −123°. The minimum-energy conformations for *si* approach are shown in structures **7a–7f**, while the lowest energy conformations for *re* approach are shown in structures **8a–8f**.

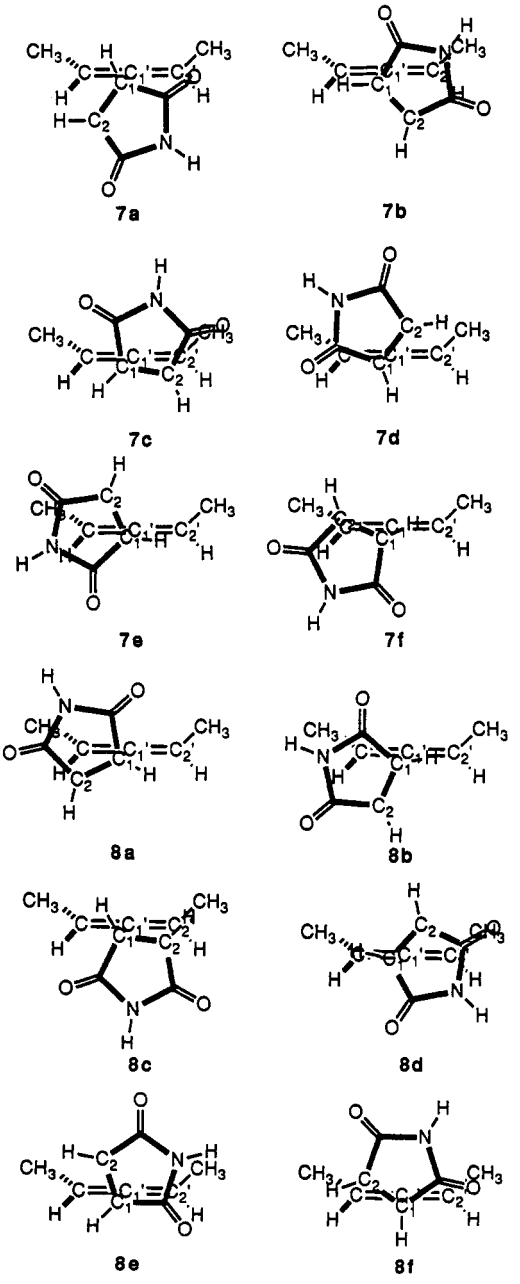

Molecular modeling calculations have also been carried out on **9** and **10** as models for the anti,anti and anti,syn diradical intermediates, in which the anti-methyl groups and the phenyl group of the NPMI have been replaced with hydrogen atoms, having both the *R* and *S* absolute

Scheme I

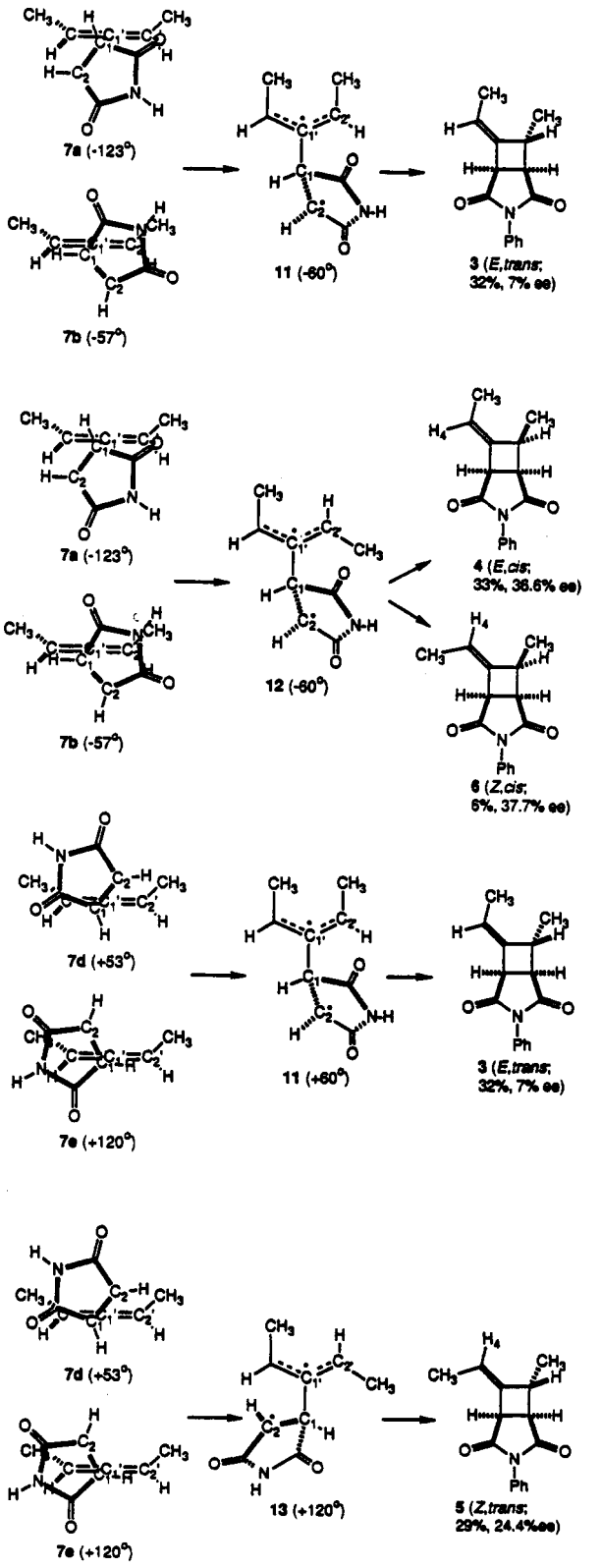

configurations at C_1 of **9** and **10**. (For steric reasons, the syn,syn diradical intermediates have not been considered to be viable intermediates[1,4] and calculations have not been

(6) The C_2–C_1–$C_{1'}$–$C_{2'}$ dihedral angles in the conformations for the approaches to the activated complexes and in the diradical intermediates are given in parentheses after the numbers of the structures.

(7) In our initial analysis of the cycloadduct distribution derived from the reaction of 13DMA with NPMI it was concluded that possibly only two minimum-energy reaction channels were required to account for the formation of all four stereoisomeric cycloadducts (see ref 4).

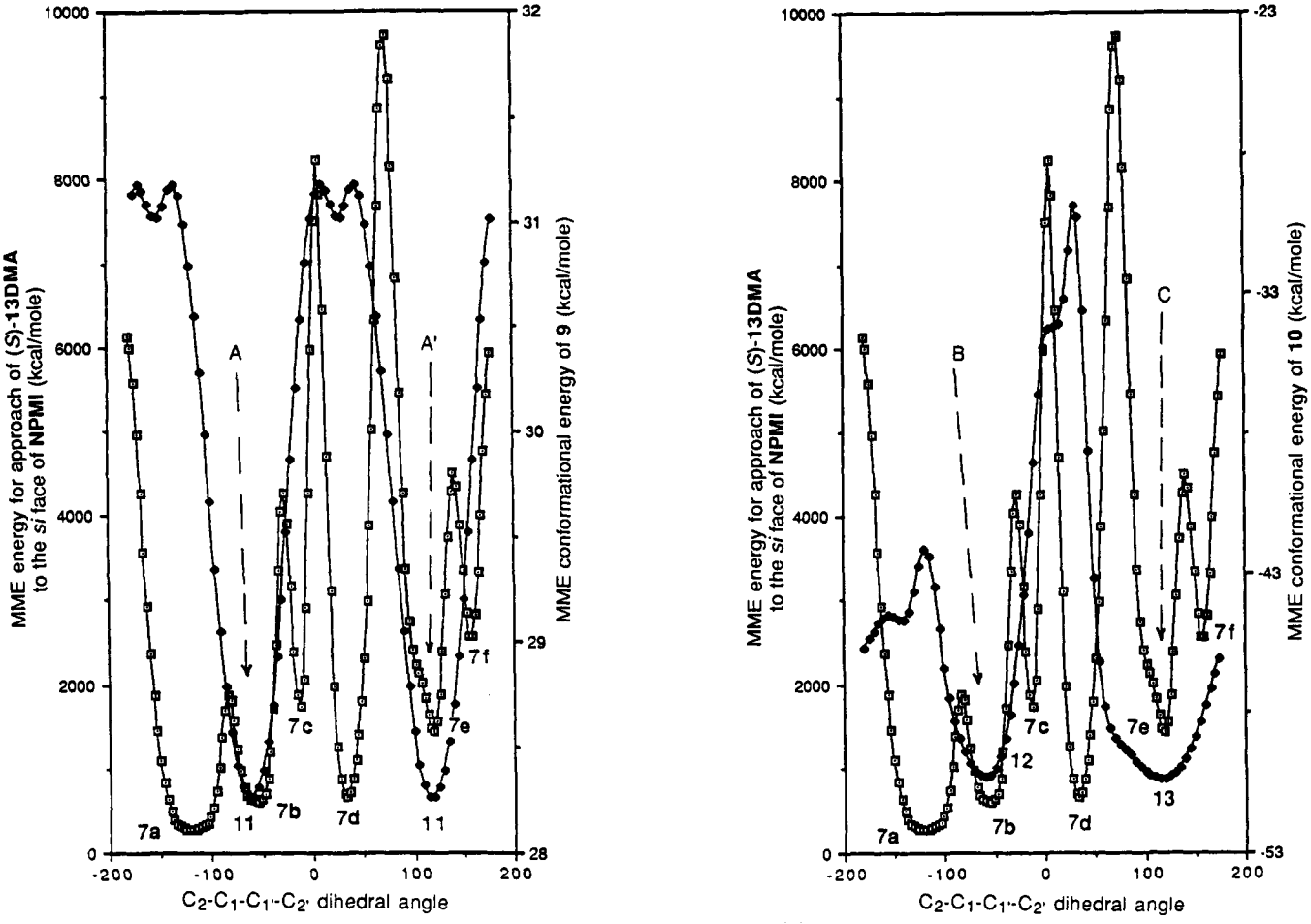

Figure 2. Plot of the energy surface for the approach of (*S*)-(+)-13DMA to the *si* face of NPMI (-⊡-) and the conformational energy surface for the anti,anti diradical intermediate model **9** (-♦-) (left). Plot of the energy surface for the approach of (*S*)-(+)-13DMA to the *si* face of NPMI (-⊡-) and the conformational energy surface for the anti,syn diradical intermediate model **10** (-♦-) (right).

carried out on those systems.) A preliminary conformational energy surface scan was carried out on **9** and **10**, and geometry optimization was then carried out on the lowest energy conformations of **9** and **10**. The final conformational energy surface was then computed for the 360° rotation about the C_2–C_1–$C_{1'}$–$C_{2'}$ dihedral angle maintaining the remaining geometry of the lowest energy optimized structures. The configurationally related energy profiles for *si* and *re* approach leading to the *R* and *S* configurations at C_2 appear in Figures 2 and 3.

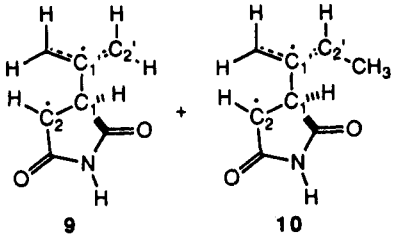

9 **10**

The lowest energy approach to an activated complex for diradical intermediate formation involves *si* attack by (*S*)-(+)-13DMA on NPMI as shown in the model **7a**.[6] Rotation of the terminal methyl group of the 13DMA away from the approaching NPMI in **7a**, along with a slight rotation about the C_1–$C_{1'}$ axis, results in the formation of intermediate **11** which is the lowest energy structure on the energy surface of **9** (see Scheme I). (The absolute configurations shown in the diradical intermediates and the cycloadducts are those produced by *si* attack on the NPMI which is calculated to be the lowest energy approach of the reactants to the activated complexes.) Alternatively, approach via **7b** only slightly higher in energy, can also lead to the formation of **11** in which only a very slight rotation about the C_1–$C_{1'}$ axis is required. These approaches to the activated comples for the formation of **11** are indicated as pathway A in the left-hand portion of Figure 2. The direct ring closure of **11** without any rotation about the C_1–$C_{1'}$ bond to one of the other minimum-energy conformations of the diradical intermediate, which would encounter an energy barrier of ~3 kcal mol^{-1}, produces cycloadduct **3** (32% yield, 7% ee). (The ee's of the cycloadducts cited for comparison purposes in this discussion are from run 5 in Table I.) Intermediate **11** can be also formed via approach **7e** (pathway A′ in the left-hand portion of Figure 2) or potentially via the lower energy approach **7d** with considerable rotation about the C_1–$C_{1'}$ axis. Both of these pathways are considerably higher in energy compared to that for the formation of **11** via pathway A and are not expected to contribute much to product formation. The ee of intermediate **11** formed via the two pathways is not expected to be the same because they are formed via two different energy conformations of the reactants in approaching the activated complexes for the formation of **11**.

The rotation of the terminal methyl group of the 13DMA toward the NPMI in **7a** or **7b** produces the minimum-energy intermediate **12** (pathway B in the right-hand portion of Figure 2). Intermediate **12** differs from **11** only in the stereochemistry about the allyl-radical portion of the intermediates. Intermediates **11** and **12** are formed from transition states that differ in structure and total energy and, thus, are not expected to be formed with

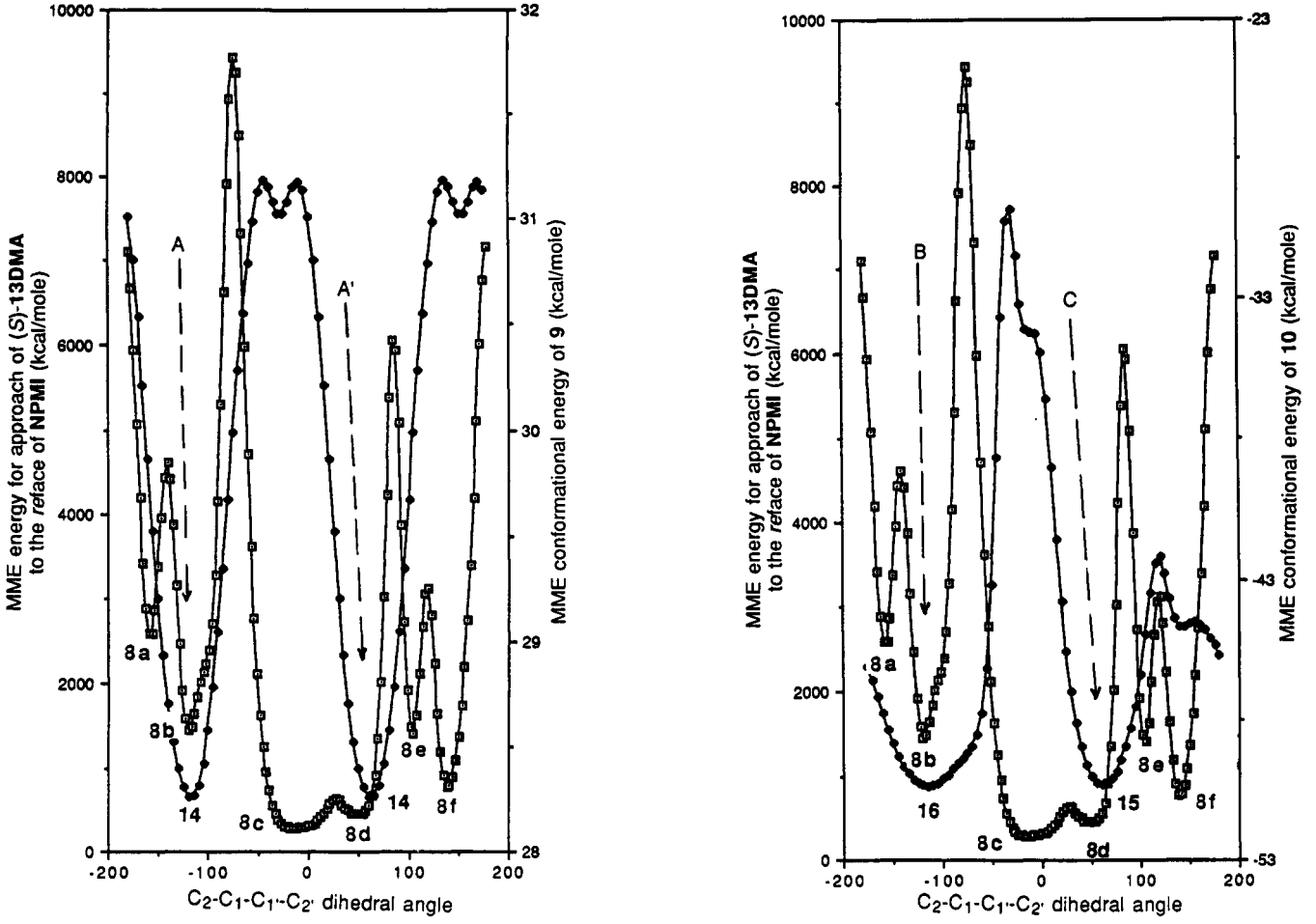

Figure 3. Plot of the energy surface for the approach of (*S*)-(+)-13DMA to the *re* face of NPMI (-⊡-) and the conformational energy surface for the anti,anti diradical intermediate model **9** (-♦-) (left). Plot of the energy surface for the approach of (*S*)-(+)-13DMA to the *re* face of NPMI (-⊡-) and the conformational energy surface for the anti,syn diradical intermediate model **10** (-♦-) (right).

the same degree of transfer of the ee of the 13DMA to the diradical intermediates. The least motion ring closure of **12** produces **4** (33% yield, 36.6% ee) and, by a low-energy, clockwise rotation about the C_1–$C_{1'}$ bond, which results in the relief of steric strain in the diradical intermediate, produces **6** (6% yield, 37.7% ee). The same ee's of **4** and **6**, within experimental error, strongly suggest their formation from a common intermediate. The much lower yield of **6** would be totally consistent with a more rapid ring closure to form **4** compared to undergoing conformational isomerization by rotation about the C_1–$C_{1'}$ bond followed by ring closure to form **6**.

The reaction of NPMI with (*S*)-(+)-13DMA via the approaches shown in **7e** or **7d** leads directly to the formation of the minimum-energy intermediate **13** by rotation of the methyl group toward the approaching NPMI (pathway C illustrated in the right-hand portion of Figure 2). The least motion ring closure of **13** results in the formation of cycloadduct **5** (29% yield, 24.4% ee). The two different rotational motions of the terminus of the 13DMA on forming the intermediates **11** and **13** from **7e** and/or **7d** give rise to intermediates differing in structure and total intrinsic asymmetry, the results of which are evident in the differences in the ee's of the cycloadducts.

The formation of the four cycloadducts **3**–**6** can be also outlined in a similar manner from approaches involving *re* attack on the NPMI with formation of the *S* configuration at C_1 in the diradical intermediates as shown in Scheme II. However, the processes going through **8b** leading to the formation of **14** and **16** and **8d** to **15**, which are enantiomeric with **11**–**12**, are higher in energy than the corresponding processes involving *si* attack, leading to the prediction that these reaction channels will result in less product formation than those proceeding via **7a**–**d** and that the predominant configuration at the C_2 of the cycloadducts formed in the cycloaddition reaction with (*S*)-(+)-13DMA is *R*.

Cycloaddition of Enantioenriched (*S*)-(+)-13DMA with Dimethyl Fumarate (DMFM). The attempted cycloaddition of 13DMA with DMFM in dilute toluene-d_8 solution, as accomplished with the cycloaddition of 13DMA with NPMI described above, resulted only in the isolation of the cycloadduct of 1,3-pentadiene with DMFM.[1,8] However, when the cycloaddition reaction is run in more concentrated solutions, the second-order cycloaddition process predominates over the first-order sigmatropic rearrangement of 13DMA to 1,3-pentadiene. Because of this, however, it was not possible to run the cycloaddition reaction under conditions where the extent of the cycloaddition reaction could be monitored, and to recover any unreacted 13DMA in order to determine its ee. However, the fact that one of the cycloadducts (**20**) is formed possessing >96% of the ee of the starting 13DMA is suggestive that the formation of the diradical intermediates in this reaction is also irreversible.

(8) A similar [1,3]-hydrogen sigmatropic rearrangement has been fully characterized in the rearrangement of 1-*tert*-butyl-3-methyallene to 1-*tert*-butyl-1,3-butadiene (Pasto, D. J.; Brophy, J. *J. Org. Chem.* **1991**, *56*, 4554.

The cycloaddition reaction of DMFM with enantioenriched (*S*)-(+)-13DMA produces a mixture of the four cycloadducts **17–20** which could be partially separated by preparative GLC (see Experimental Section).[9] The ee's of the cycloadducts **18** and **20** could be determined readily by the use of an europium NMR chiral shift reagent resulting in base-line resolution of the ester methyl groups. Only one value for the ee of cycloadduct **17** could be obtained. Insufficient quantities of **19** of necessary purity prevented the measurement of its ee. Two runs were carried out with different starting ee's of the 13DMA. The ee's of the starting 13DMA in the two runs are indicated under its structure in the following equation, with percent yields and ee's of the cycloadducts being indicated in parentheses as (% yield run 1, % yield run 2; % ee run 1, % ee run 2). The major cycloadduct **20** is formed with >96% transfer of the ee of the 13DMA, while cycloadducts **17** and **18** are formed with 74 and 69% transfer of the ee of the 13DMA. In view of the apparent irreversibility of formation of the diradical intermediates, this data demands that more than a single minimum-energy reaction pathway is involved in formation of the products.

Scheme II

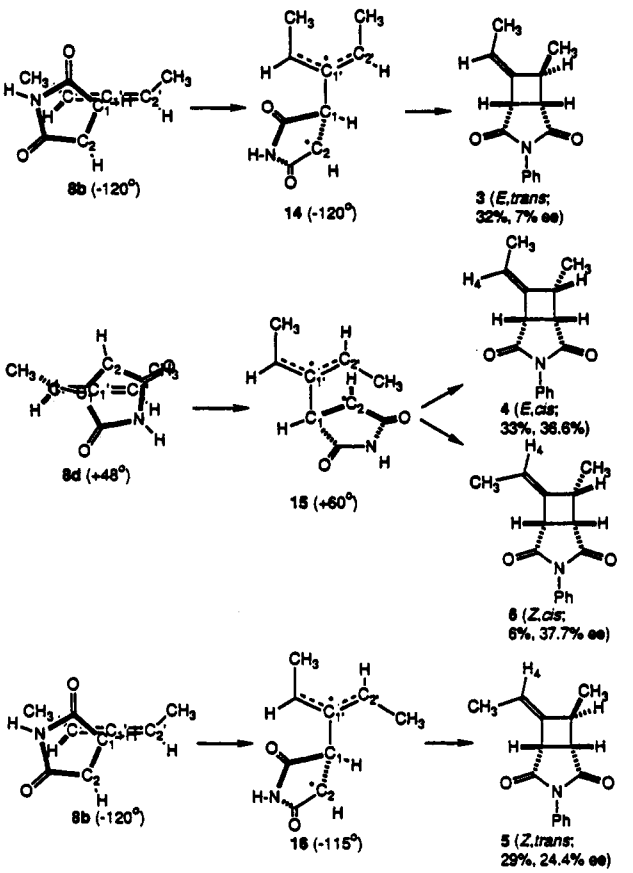

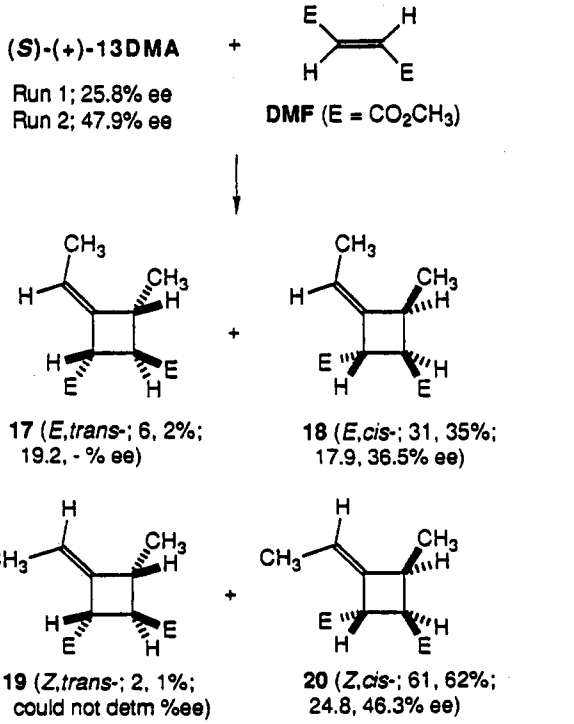

(9) The cis and trans stereochemical relationships between the C_4-methyl and C_3-ester functions have been reversed compared to that suggested in our earlier structural study on the cycloadducts formed from 13DMA and diethyl fumarate[1] in which the stereochemistry of the cycloadducts was assigned on the basis of the relative chemical shifts of the proton at C_4 and the relative magnitudes of the vicinal coupling constants between the protons attached to C_2 and C_3 and C_3 and C_4. It was assumed that the long-range shielding effects on the chemical shifts of the protons attached to C_4 were negligible and that the presence of all of the functionality on the four-membered ring did not have a significant perturbing influence on the conformation of the four-membered ring which would affect the relative magnitudes of the chemical shifts or on the vicinal coupling constants. The results of molecular modeling calculations on the minimum-energy reaction channels described immediately following, however, indicate that the trans cycloadducts, previously proposed as the major set of cycloadducts,[1] cannot be formed as the major cycloadducts out of any of the minimum-energy reaction channels for either *si* or *re* face attack on the DMFM. Molecular mechanics optimization calculations on the two conformations of **17**, **18**, and **20** indicate conformational preferences not anticipated in the original article produce dihedral angles between the vicinally related hydrogen atoms on C_2, C_3 and C_4 which are more consistent with the observed vicinal coupling constants. Geometry optimization calculations have been carried on the two possible conformations of **17**, **18**, and **20** (cycloadduct **19** was not obtained in sufficient quantity or purity to derive its coupling constants, ref 1) using MACROMODEL program, V2.5 (Still, W. C.; Mohamadi, F.; Richards, N. G. J.; Guida, W. C.; Lipton, M.; Liskamp, R.; Chang, G.; Hendrickson, T.; DeGunst, F.; Hasel, W. MacroModel V2.5; Department of Chemistry, Columbia University, New York, NY 10027). The only minimum-energy conformation located for **18** is that shown as **18eea** in which the two ester functions (*E*) are oriented pseudoequatorially with the methyl group at C_4 essentially eclipsed with the syn vinyl methyl group, a orientation that is not favored in the nondiester parent system.[4] The preference for the two ester groups to be oriented pseudoequatorially must overcome the repulsion energy between the two methyl groups in **18eea**. The H_1–C_4–C_3–H_2 and H_2–C_3–C_2–H_4 dihedral angles of 12.2° and 149.9° are completely consistent with the observed vicinal coupling constants of 9.90 and 7.90 Hz, respectively. Two minimum-energy conformations were located for **20** with **20eea** being slightly lower in energy than **20aae**. In **20aae** the two ester functions are oriented pseudoaxially with the methyl group being oriented pseudoequatorial. In the higher energy conformation **20eea**, the ester function attached to C_2 is essentially "eclipsed" with the syn vinyl methyl group. This interaction must be similar in magnitude with that having the two esters pseudoequatorial with the C_4 methyl pseudoaxial. The H_1–C_4–C_3–H_2 and H_2–C_3–C_2–H_4 dihedral angles in **20eea** are calculated to be 8.8 and 147.2°, and in **20aae**, 20.2 and 115.7°. The observed coupling constants are 10.57 and 5.28 Hz, again consistent with time-averaged coupling constants expected for the calculated dihedral angles. Only a single minimum-energy conformation could be located for **17**, that being **17eee** with all of the groups being oriented pseudoequatorially. The H_1–C_4–C_3–H_2 and H_2–C_3–C_2–H_4 dihedral angles are 142.1 and 141.5°. The observed H_1–H_2 vicinal coupling constant of 3.30 Hz is much smaller than that in **18** and **20** and is consistent with the relative magnitude of the H_1–C_4–C_3–H_2 dihedral angle and the reassignment of the ring stereochemistry of the cycloadducts.

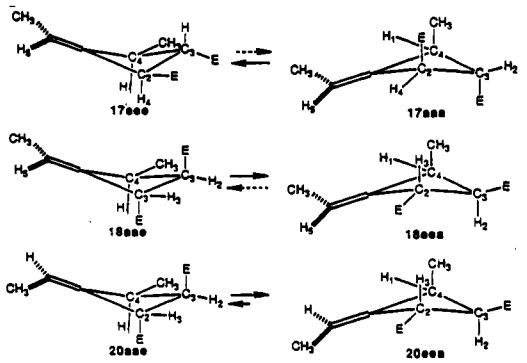

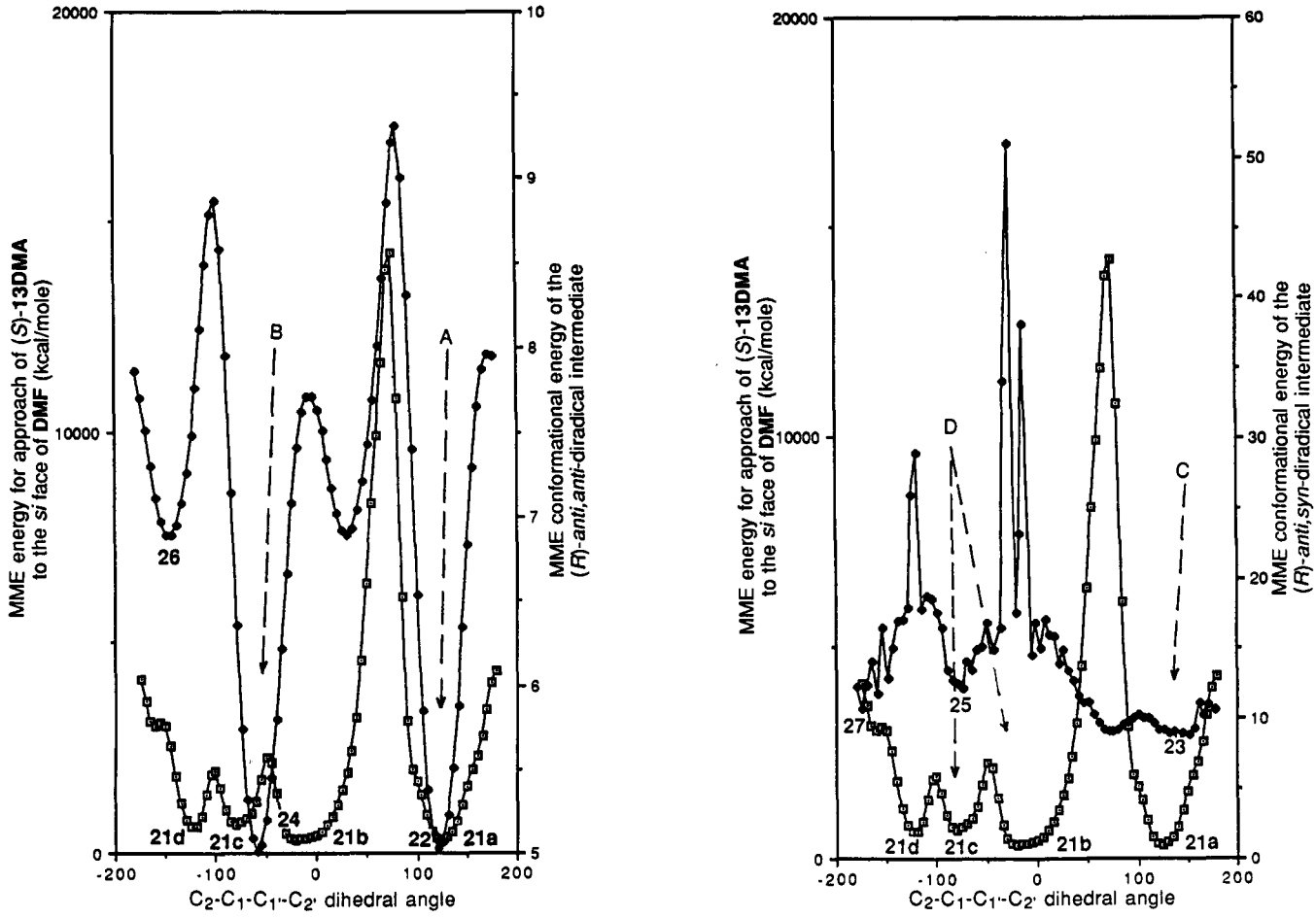

Figure 4. Plot of the energy surface for the approach of (*S*)-(+)-13DMA to the *si* face of DMFM (-⊡-) and the conformational energy surface for the anti,anti diradical intermediate model **9** (-♦-) (left). Plot of the energy surface for the approach of (*S*)-(+)-13DMA to the *si* face of DMFM (-⊡-) and the conformational energy surface for the anti,syn diradical intermediate model **10** (-♦-) (right).

In order to analyze the stereochemical details of the formation of the cycloadducts, molecular modeling calculations have been carried out on the conformational energy surface for the approach of the reactants to the activated complexes and on the diradical intermediates using the Chem-X suite of programs.[5] In these calculations the ester methyl groups and the anti methyl groups in the diradical intermediates have been replaced by hydrogen atoms. The lowest energy conformation of DMFM was first located and optimized and then "docked" to the optimized structure of 13DMA using the molecular fitting routine of the Chem-X program such that the axes of the 2p AO's on C_1 of the DMFM and $C_{1'}$ of the 13DMA were coincident with a C_1–$C_{1'}$ separation distance of 2.00 Å for both *re* and *si* face approach to C_1 of the DMFM. An energy surface scan was then carried out by rotation through 360° about the C_2–C_1–$C_{1'}$–$C_{2'}$ dihedral angle. No attempts have been made to optimize the minimum-energy conformations for the approaches of the reactants to the activated complexes. The results of these conformational energy surface scans are shown in Figures 4 and 5. MME conformational energy surface scan calculations have also been carried out on models for the diradical intermediates possessing the *R* and *S* configurations at C_1. An initial conformational energy surface scan was carried out on unoptimized structures for the anti,anti and anti,syn diradical intermediate models. Optimization was then carried out on the lowest energy conformation for the two enantiomerically related diradical intermediates, and then a conformational energy surface was calculated for those optimized structures by carrying out a 360° rotation about the C_2–C_1–$C_{1'}$–$C_{2'}$ dihedral angle maintaining the remaining geometrical parameters of the optimized intermediates. The energy scan plots are shown in Figures 4 and 5. The lowest energy conformations for the approach to the activated complexes for *si* attack on the DMFM are those shown in **21a–d** in Scheme III resulting in the formation of the *S* configuration (the C_2–C_1–$C_{1'}$–$C_{2'}$ dihedral angles are given in parentheses), which are considerably lower in energy than those for *re* approach resulting in the formation of the *R* configuration.

The lowest energy reaction channel involves the approach of the DMFM to the (*S*)-(+)-13DMA as illustrated in **21a** in Scheme III. Bond formation with rotation of the methyl of the 13DMA away from the approaching DMFM directly results in the formation of **22** possessing the *S* configuration (which is also that predicted to be present in the cycloadducts) and which represents a minimum-energy conformation on the energy surface of the anti,anti diradical intermediate having a C_2–C_1–$C_{1'}$–$C_{2'}$ dihedral angle essentially identical with that of **21a** (pathway A in the left-hand portion of Figure 4). The least motion ring closure of **22** produces the *E*,cis cycloadduct **18**. Rotation about the C_1–$C_{1'}$ bond in **22** to produce another minimum-energy conformation capable of undergoing ring closure to one of the other stereoisomeric cycloadducts is not probable, the energy barrier of ~3 kcal mol^{-1} for such a rotation appearing to be appreciably greater than that for ring closure.[4] Rotation of the methyl group toward the approaching DMFM, along with a small rotation about the C_1–$C_{1'}$ axis, produces **23**, which also represents a minimum-energy conformation of the anti,syn diradical in-

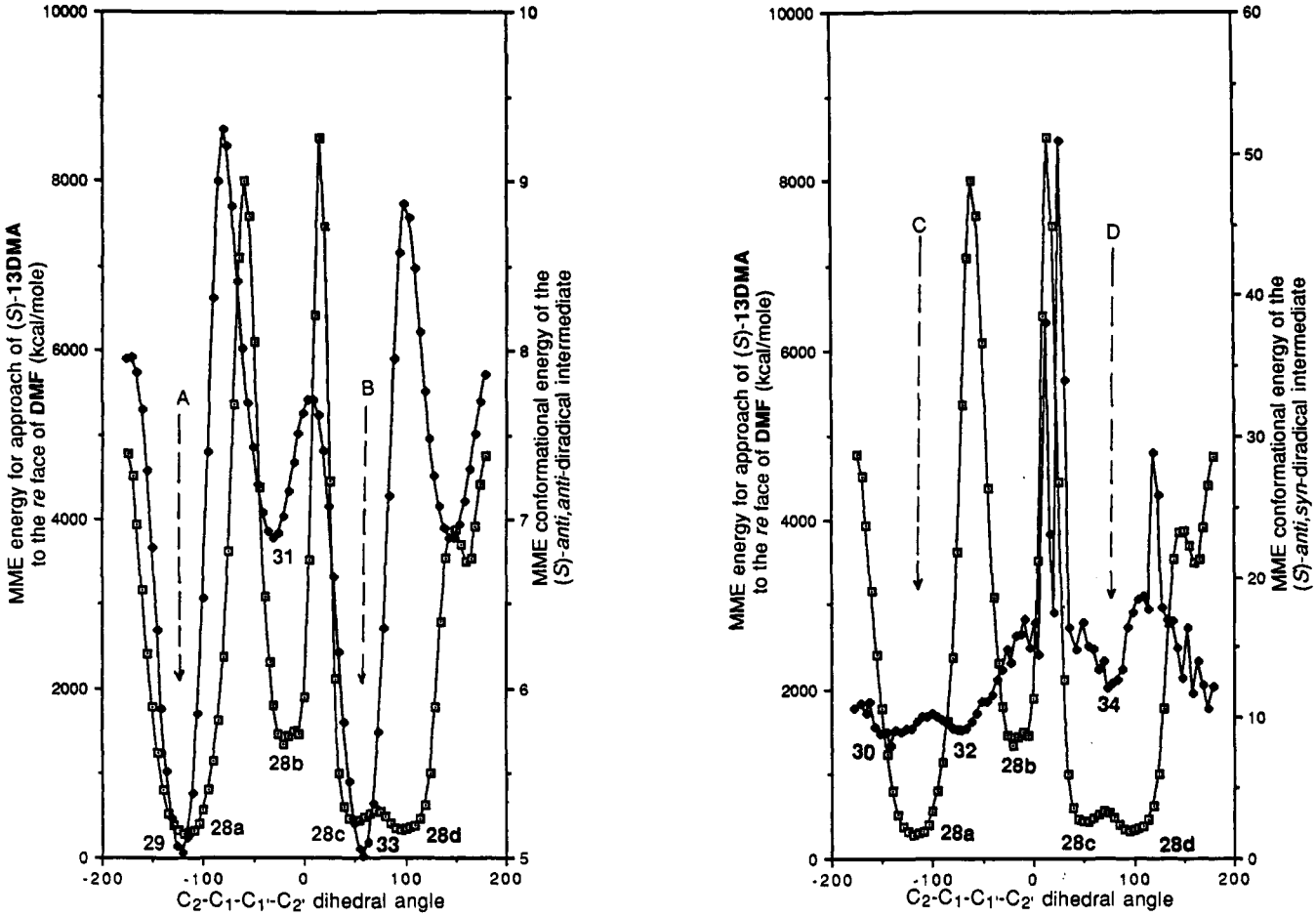

Figure 5. Plot of the energy surface for the approach of (*S*)-(+)-13DMA to the *re* face of DMFM (-⊡-) and the conformational energy surface for the anti,anti diradical intermediate model **9** (-♦-) (left). Plot of the energy surface for the approach of (*S*)-(+)-13DMA to the *re* face of DMFM (-⊡-) and the conformational energy surface for the anti,syn diradical intermediate model **10** (-♦-).

termediate (pathway C in the ring-hand portion of Figure 4). The least motion ring closure of **23** produces the major *Z*,cis cycloadduct **20**. Although both **18** and **20** are formed via the same initial conformation in the approach of the reactants to the activated complexes, the transition states for formation of **22** and **23** differ in structure and energy and would be expected to result in different degrees of asymmetric induction during formation of the diradical intermediates.

The approaches illustrated in **21b** and **21c** result in the formation of intermediates **24** and **25** (pathways B and D in Figure 4) and, in turn, the cycloadducts **18** and **17**, respectively. The reaction channels proceeding through **21b** and **21c** are considerably higher in energy compared to the reaction channel proceeding via **21a** and would not be expected to contribute significantly to product formation. It is interesting to point out, however, that this is the only reaction channel involving *si* attack in which the very minor *E*,trans cycloadduct **17** can be formed.

The second lowest energy reaction channel involves the approach illustrate in **21d** resulting in the formation of the minimum-energy conformations of the diradical intermediates **26** and **27**. The least motion ring closure of **26** produces **17**. This reaction channel is the only pathway that leads to the formation of the very minor cycloadduct **19** via *si* attack on the DMFM.

In summary, the lowest energy reaction channel proceeding via the approach shown in **21a** leads directly to the two major cycloadducts **18** and **20**. Cycloadduct **18** can also be formed via approach **21b**, but this pathway is considerably higher in energy and is not expected to contribute significantly to the formation of **18**. The very minor cycloadduct **17** can only be formed via **21b**, while the other very minor cycloadduct **19** can only be formed via approach **21d**, which is also a very high energy pathway.

An analysis of the various approaches for *re* attack of the 13DMA on the DMFM, resulting in the formation of the *R* configuration at the newly formed stereogenic center, leads to the same conclusions in terms of what reaction channels lead to each of the cycloadducts, all ultimately differing only in the absolute configurations in the cycloadducts. On the basis of our earlier success in being able to predict the correct absolute configurations in the cycloadducts formed in the (2 + 2) cycloaddition reaction of (*R*)-(-)-13DMA with acrylonitrile,[4] it is felt that the results of the molecular modeling calculations on the cycloaddition pathways for the reaction of 13DMA with DMFM also provides for an adequate prediction of the configurations in the cycloadducts formed in this reaction.

Summary

The irreversible formation of the diradical intermediates in the (2 + 2) cycloaddition reactions of 13DMA with NPMI and DMFM occurs with a very high degree of transfer of the ee of the 13DMA (asymmetric induction) to the newly formed stereogenic center in the diradical intermediates. These observations open up the possibility for the use of enantioenriched chiral allenes in the synthesis of interesting structures in which a new saturated

Scheme III

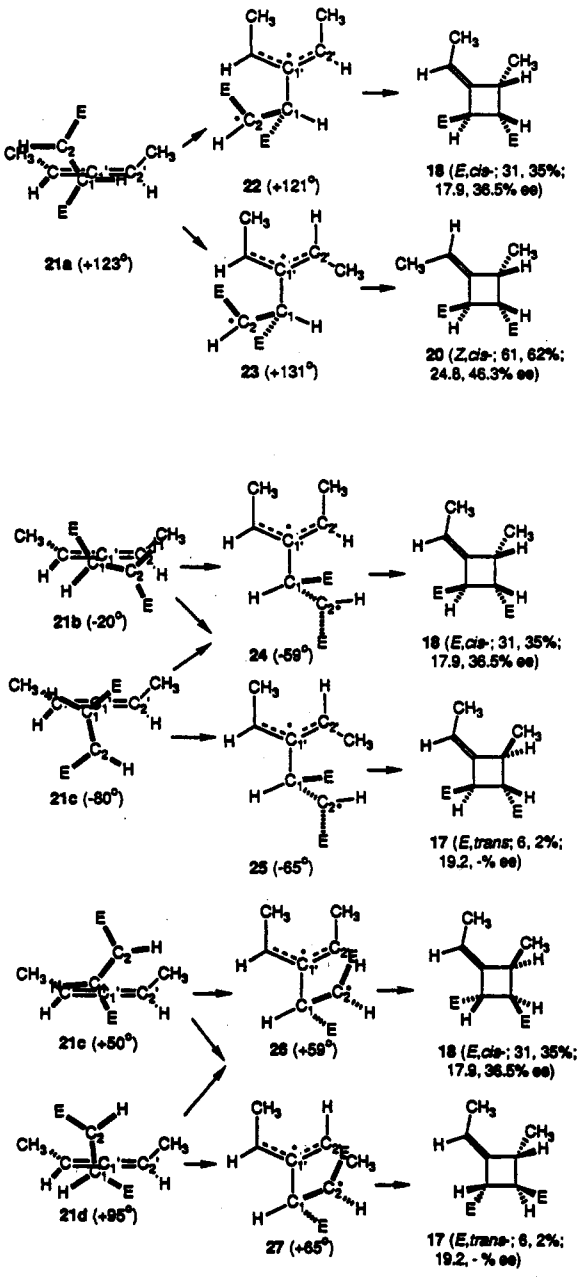

stereogenic center is formed during the addition to the central allene carbon. Studies are currently being carried out to explore these possibilities.

Experimental Section

Cycloaddition of Enantioenriched (*S*)-(+)-13DMA with NPMI. In an NMR tube were placed the (*S*)-(+)-13DMA, NPMI, and toluene-d_8. The quantities of each and the rotation of the 13DMA in the five runs follow. (The α's have been measured at 589 nm at 25 °C.) Run 1: 140 mg (2.06 mmol) of 13DMA with $\alpha = 0.817 \pm 0.001°$ ($c = 0.825$ in diethyl ether, 27.1% ee), 178 mg (1.03 mmol) of NPMI, 500 μL of toluene-d_8. Run 2: 140 mg (2.06 mmol) of 13DMA with $\alpha = 0.152 \pm 0.001°$ ($c = 0.620$ in diethyl ether, 30.3% ee), 178 mg (1.03 mmol) of NPMI, 500 μL of toluene-d_8. Run 3: 140 mg (2.06 mmol) of 13DMA with $\alpha = 0.152 \pm 0.001°$ ($c = 0.620$ in diethyl ether, 30.3% ee), 178 mg (1.03 mmol) of NPMI, 500 μL of toluene-d_8. Run 4: 35 mg (0.52 mmol) 13DMA with $\alpha = 0.120 \pm 0.001°$ ($c = 0.460$ in diethyl ether, 32.3% ee), 88 mg (0.52 mmol) of NPMI, 1.70 mL of toluene-d_8. Run 5:: 140 mg (2.06 mmol) of 13DMA with $\alpha = 0.355 \pm 0.001°$ ($c = 0.915$ in diethyl ether, 47.9% ee), 178 mg (1.03 mmol) of NPMI, 500 μL of toluene-d_8. The contents of the tube were triply freeze–degassed, sealed under a vacuum, and heated in a sand bath at 160 °C. The NMR spectrum was recorded periodically. After the complete disappearance of the NPMI, the tube was opened and the volatiles were removed on a vacuum line. The unreacted 13DMA was recovered by preparative GLPC on a 12 ft × $^1/_4$ in. 20% SE-30 on Chromosorb P column at 90 °C. The rotations of the recovered fractions of 13DMA were recorded giving the following values. Run 1: $\alpha = 0.384 \pm 0.001°$ ($c = 1.750$ in diethyl ether, 27.1% ee). Run 3: $\alpha = 0.182 \pm 0.001°$ ($c = 0.770$ in diethyl ether, 29.2% ee). Run 5: $\alpha = 0.719 \pm 0.001°$ ($c = 2.050$ in diethyl ether, 43.3% ee). Insufficient 13DMA was recovered from runs 2 and 4 to record its rotation.

The mixture of cycloadducts was separated by preparative HPLC on a 200 × 4.6 mm silica gel column using a 90:10 mixture of hexane–ethyl acetate. (The NMR data of **3–6** have been reported in ref 1.) The ee's of **3–6** were determined by the addition of aliquots of a solution of tris[3-(trifluoromethylhydroxymethylene)-(+)-camphorato]ytterbium(III) dissolved in $CDCl_3$ until near base-line resolution of the vinyl proton resonances was obtained while saturating the vinyl methyl resonance. The ee's were calculated from the integrals obtained from the NMR spectra and are given in Table I.

Cycloaddition of (*S*)-(+)-13DMA with DMFM. In an NMR tube were placed the (*S*)-(+)-13DMA, DMFM, and toluene-d_8. The quantities of each and the rotations of the 13DMA for the two runs follow. Run 1: 70 mg (1.03 mmol) of 13DMA with $\alpha = 0.261 \pm 0.001°$ ($c = 1.25$ in diethyl ether, 25.8% ee), 148 mg (1.03 mmol) of DMFM, 100 μL of toluene-d_8. Run 2: 70 mg (1.03 mmol) of 13DMA with $\alpha = 0.355 \pm 0.001°$ ($c = 1.25$ in diethyl ether, 47.9% ee), 148 mg (1.03 mmol) of DMFM, 100 μL of toluene-d_8. The contents of the tube were triply freeze–degassed, and the tube was sealed under vacuum. The tube was heated in a sand bath at 160 °C for 5 d. The tube was opened, and the solvent was removed on a vacuum line. The ^{1}H NMR spectrum of the residue indicated the formation of only the four cycloadducts **17–20**. There was no evidence for the formation of any polymeric materials. The mixture of the four cycloadducts was partially separated by preparative GLC on a 12 ft × $^1/_4$ in. 20% TCEP on Chromosorb column at 160 °C giving a pure fraction of cycloadduct **18** and a mixture of cycloadducts **17** and **20**. Cycloadduct **19** could not be isolated in quantities suitable for analysis.

17: ^{1}H NMR ($CDCl_3$) δ 1.34 (d, $J = 6.88$ Hz, 3 H), 1.59 (ddd, $J = 7.05, 2.62, 2.30$ Hz, 3 H), 3.18 (m, 1 H), 3.68 (m, 1 H), 3.72 (s, 3 H), 3.73 (s, 3 H), 3.86 (qdd, $J = 7.54, 2.62, 2.62$ Hz, 1 H), 5.47 (qdd, $J = 7.05, 2.62, 2.62$ Hz, 1 H).

18: ^{1}H NMR ($CDCl_3$) δ 1.13 (d, $J = 7.25$ Hz, 3 H), 1.56 (ddd, $J = 6.99, 2.48, 1.39$ Hz, 3 H), 3.36 (dqdq, $J = 9.94, 7.25, 2.89, 1.39$ Hz, 1 H), 3.60 (dd, $J = 9.94, 7.98$ Hz, 1 H), 3.71 (s, 3 H), 3.72 (s, 3 H), 4.17 (dq, $J = 7.98, 2.48$ Hz, 1 H), 5.48 (qdd, $J = 6.99, 2.89, 2.54$ Hz, 1 H); HR EIMS calcd for $C_{11}H_{16}O_4$, 212.1049, found 212.1050.

19: ^{1}H NMR ($CDCl_3$) (from the NMR spectrum of the crude reaction product) δ 1.28 (3 H), 1.57 (3 H), 3.04 (1 H), 3.60 (3 H), 3.95 (3 H), 5.32 (1 H).

20: ^{1}H NMR ($CDCl_3$) δ 1.04 (d, $J = 7.06$ Hz, 3 H), 1.60 (ddd, $J = 6.92, 2.36, 1.70$ Hz, 3 H), 3.43 (dqdq, $J = 10.41, 7.07, 2.70, 2.36$ Hz, 1 H), 3.57 (dd, $J = 10.41, 5.37$ Hz, 1 H), 3.70 (s, 3 H), 3.71 (s 3 H), 4.17 (dqd, $J = 5.37, 1.70, 1.43$ Hz, 1 H); 5.35 (qdd, $J = 7.06, 2.70, 1.43$ Hz, 1 H); HR EIMS calcd for $C_{11}H_{16}O_4$, 212.1049, found 212.1048.

The ee's of **17**, **18**, and **20** were determined by the addition of aliquots of a solution of tris[3-(trifluoromethylhydroxymethylene)-(+)-camphorato]europium(III) dissolved in $CDCl_3$ to the NMR samples until base-line resolution of the ester methyl resonances was obtained. The ee's were calculated directly from the integrals of the ester methyl region in the NMR spectra and are given under the structures for the two runs.

Acknowledgment. We acknowledge the National Science Foundation for support of this research (NSF No. CHE8709725).